Proceedings of FEDSM'98
1998 ASME Fluids Engineering Division Summer Meeting
June 21–25, 1998, Washington, DC

FEDSM98-4868

NUMERICAL INVESTIGATION OF THE BLADE COOLING EFFECT GENERATED BY MULTIPLE INCOMPRESSIBLE JETS

Subrata Roy and Panos Tamamidis
Case Corporation
7S. 600 County Line Road
Burr Ridge, IL 60521-6975, USA

ABSTRACT

The thermal effect of cool jets issuing into an incompressible hot cross flow at an angle over a turbine blade is the subject. Numerical solutions using the k-ε turbulence closure model for eight multiple hole arrangements with three different hole spacings and three different jet issuing angles document strong to moderate secondary vortex structures spanning normal to the direction of the jet. This fully three dimensional flow field strongly influences the cooling performance of the hole-blade system. For a generalized body-fitted three dimensional finite element model, computational results suggest an *optimum* hole spacing and low issuing angle for maximum cooling efficiency.

INTRODUCTION

The interaction of cool air jets with hot crossflow generates complex flowfields which exist in a variety of industrial applications including V/STOL engineering, film cooling of turbine blades, jets into combustors, and waste disposal from smoke stacks into the atmosphere. Systematic investigation of such flowfield under isothermal condition began several decades ago [1-4]. Numerical investigations of jets were initially based on integral methods and essentially idealized models [5-7]. A number of numerical models have also been proposed that approximated the three-dimensional vortex sheet by a two-dimensional one to predict details of the flowfield [7]. However, the mixing of a jet in a cross-stream is a three-dimensional phenomenon [3], and thus such idealized treatments lack accuracy.

Numerical solutions of the full Navier-Stokes equations have also been used to obtain detailed solutions in various studies. Early attempts [8] used closure models based on constant turbulent viscosity. One of the serious problems affecting the flow predictions is the selection of the turbulence model [9]. Recent studies were based on the k-ε model of turbulence or its variants. The results of these studies indicate that the k-ε model gives predictions of engineering accuracy, and that such predictions depend on the blow ratio R (by blow ratio we mean the ratio of the mean flow velocities in the injection pipe and the wind tunnel) and the distance downstream from the injection holes. Non-isotropic models, based on algebraic expressions for the Reynolds stresses have also been used [10,11]. Although the results were improved for some R, there were cases where the standard k-ε model still yielded better results. Recently the three dimensional isothermal secondary vortex structure was examined [12] using three different finite volume (FV) schemes and a two equation turbulence closure model for single and multiple jets issuing at 45° to the wind tunnel for R=3.

As a complement to [12], the focus of this work is to investigate the thermal effect of the complex flow field generated by the injection of multiple jets of spacing L issuing at an angle $\alpha \leq 45°$ into an incompressible cross-flow. The cases examined here correspond to $R \leq 3$ which is mostly important to turbomachinery flows. The cooling performance of four different arrangements of holes with a combination of L and α are analyzed using a upwind biased linear basis finite element code and standard k-ε turbulence closure model. Numerical solutions using the k-ε turbulence closure model for four multiple hole arrangements with a combination of different hole spacings L and jet issuing angle α document strong to moderate secondary vortex structures spanning normal to the direction of the jet. This fully three dimensional flow field strongly influences the cooling performance of the hole-blade system. Computational results show an *optimum* hole spacing and low issuing angle for maximum cooling efficiency.

THEORETICAL FORMULATION

Governing Equations

The transformation of the system of equations for steady, turbulent, buoyancy-driven, incompressible flows, including the k-ε model, has been studied in detail in the literature [7]-

[12]. For state variable $[u \quad v \quad w \quad k \quad \varepsilon \quad T]^T$, the transformed equations for the intrinsic coordinate system ξ_i can be written as

$$\frac{\partial \mathbf{E}^{\xi_i}}{\partial \xi_i} = \frac{\partial}{\partial \xi_i}\left(\mathbf{E}_v^{\xi_i} + \hat{\mathbf{E}}_v^{\xi_i}\right) + \mathbf{S} \tag{1}$$

where

$$\mathbf{E}^{\xi_i} \equiv \rho U^{\xi_i}\begin{bmatrix}1 & u & v & w & k & \varepsilon & T\end{bmatrix}^T \tag{2}$$

$$\mathbf{E}_v^{\xi_i} = \Gamma_{eff} g^{\xi_i \xi_i} \frac{\partial}{\partial \xi_i}\begin{bmatrix}1 & u & v & w & k & \varepsilon & T\end{bmatrix}^T \tag{3}$$

$$\hat{\mathbf{E}}_v^{\xi_i} = \Gamma_{eff} g^{\xi_i \xi_j} \frac{\partial}{\partial \xi_j}\begin{bmatrix}1 & u & v & w & k & \varepsilon & T\end{bmatrix}, i \neq j \tag{4}$$

and $\mathbf{S}$ is the source term which includes Boussinesque approximation for the momentum equation. In the above equations $U^{\xi i}$ is the scaled ξ_i component of the contravariant velocity vector, and $g^{\xi_i \xi_j}$ are metric components introduced from the transformation of the equations from the physical (x,y,z) to the computational (x,h,z) space:

$$U^{\xi_i} = Ja\left(u_j \frac{\partial \xi_i}{\partial x_j}\right), (5) \text{ and } g^{\xi_i \xi_j} = Ja\left(\frac{\partial \xi_i}{\partial x_k}\frac{\partial \xi_j}{\partial x_k}\right) \tag{6}$$

where Ja is the jacobian of the transformation matrix.

Turbulence Modeling

In this work, a high-Reynolds k-ε model is used. This model introduces two equations, one for the turbulent kinetic energy k and the other for its dissipation rate ε. These equations are included in the set of the transformed equations (1). The effect of this model is to introduce an additional viscosity, called turbulent viscosity, which is calculated as a function of density ρ as

$$\mu_t = C_\mu \rho \frac{k^2}{\varepsilon} \tag{7}$$

The turbulent viscosity is not a fluid property, but rather a property of the flow field. Its value is added to the molecular viscosity and yields an effective viscosity, μ_{eff}, which is used in the calculations. The various terms associated with the k-ε model are the production of turbulence G, some arbitrary constants C_i, and the effective transport coefficient G_{eff}. The latter is equal to the effective viscosity μ_{eff} for the momentum equations, while for the k- and ε–equations, is equal to μ_{eff} divided by the respective turbulent Prandtl number s. The generation of turbulence is calculated from the following equation:

$$G = \mu_t\left(\frac{\partial u_i}{\partial \xi_k}\frac{\partial \xi_k}{\partial x_j} + \frac{\partial u_j}{\partial \xi_k}\frac{\partial \xi_k}{\partial x_i}\right)\frac{\partial u_i}{\partial \xi_k}\frac{\partial \xi_k}{\partial x_j}. \tag{8}$$

Solution Procedure

Equations (1) through (4) constitute a system of non-linear algebraic equations. The system is linearized by resorting to relaxation. A streamline upwinding technique is employed for stabilizing the numerical iterations. The pressure corrections are used to correct the pressure and the velocities. This predictor-corrector procedure constitutes one iteration. The solution is declared convergent when the maximum residual for each of the state variable becomes smaller than a convergence criterion of 10^{-4}. Here, the convergence of a solution vector $\mathbf{U}$ on node n is defined as the norm:

$$\frac{\|\mathbf{U}_n - \mathbf{U}_{n-1}\|}{\|\mathbf{U}_n\|} \leq 10^{-4} \tag{9}$$

Boundary Conditions

On the bottom plate the typical wall boundary conditions are used, i.e., the no-slip condition for the velocities and the wall functions for the k and ε. Over the holes the axial (that is, along the axis of the pipe) velocity profile is prescribed, and then this is decomposed into u- and v-profiles; the w-profile assumes zero values. The k and ε are calculated from the following expressions:

$$k_{in} = \frac{3}{2}(T_u \cdot u)^2, \quad \varepsilon_{in} = \frac{k_{in}^{3/2}}{L_\varepsilon} \tag{10}$$

where T_u is the turbulence level, which is equal to the 10% in the present study. L_ε is a characteristic length of the domain, i.e. the size of the hole. In the upstream boundary, the u-velocity is prescribed a non-zero value, while the v and w components are set equal to zero. The k and ε are calculated from Eq. (10). Finally, the temperatures are prescribed as 27°C at the jets and 100°C at the wind tunnel inlet. The freestream and downstream conditions are zero gradients for all state variables.

RESULTS AND DISCUSSION

The schematic of the flow domain is shown in Fig. 1. The cool jet at 27°C is injected into the 100°C hot cross-flow with an angle $\alpha \leq 45°$. The injection ducts are circular pipes with radius equal to r=7 mm. The injection hole formed by the intersection of the injection pipe with the wind tunnel is an ellipse with the minor and the major axes r and D=r/(cos a), respectively. L is the distance between the hole centers. The mean flow velocities in the injection pipe (≤100 m/sec) and the wind tunnel (=33.33 m/sec) gives a high blow ratio R≤3. The inlet section is located at x=-5D and the exit at x=40D. The other dimensions are shown in Figure 1. Due to the symmetry of the flow field across the hot cross-flow direction (z/D=0), only half of the domain is considered for analysis.

A mesh independence study [12] between three different mesh sizes of 55,000 (55x29x36) elements, 165,000 (75x39x56) elements, and 307,000 (95x49x66) elements, Figure 2, established the moderate 165,000 elements as the

optimum mesh. The inlet conditions for this mesh study were uniform velocity profiles for both the wind tunnel and the hole exit. It should be noted here, that grid independent solution with respect to turbulence variables has not been achieved, but the difference on the results from the moderate and fine grids is negligible and use of any finer mesh would only increase the computational cost.

For better understanding of the simulations, the multiple-jet flowfield can be divided into three areas: (i) The central jet, (ii) the outside jet and (iii) the internal region. The jets coming out of the pipes appear to the incoming tunnel flow as "solid". A sharp velocity and temperature gradient is formed upstream of the jet while a "wake" region develops downstream of the jet. In the latter a pair of bound vortices per jet is formed, which bends the jet, producing the well known kidney shape both in speed and temperature line contours, Figure 3. The stronger the vortices, the more distorted the jet cooling effect becomes.

Figure 4 shows the general trend of the u-profiles at several cross-sectional stations and on three planes: z/D=0 (symmetry plane), z/D=2 (half-distance between the two-jets), and z/D=4.2 (center-plane of the outside jet). At x/D=1.5 the velocity distributions in the central planes of the two jets are very comparable. However, this starts changing slowly from x/D=2.5, indicating that the interaction between the two jets has started. The double peak in the velocity profiles at z/D=0 and z/D=4.2 confirms a large wake region in the lee of the jet associated with a low back pressure, which causes flow motion towards the symmetry planes of the jets. This inward motion is more pronounced close to the wall, and is also augmented by the bound vortex motion. Thus, high-momentum fluid is carried from the cross-stream to the symmetry planes causing the maxima of u-velocity near the and like the single-jet case, suggests that the flow near the wall has wall-jet character. The difference with the single-jet case is that in the multiple-jet case the row of jets presents a larger obstacle to the freestream flow. The back pressure is smaller, causing the jets to bend more than in the single-jet case. There is also a transverse pressure gradient, with higher pressures in the central plane of the outside jet than in the central plane of the middle jet. This transverse pressure gradient causes the asymmetries in the development of the two jets. At x/D=4.5 the interaction between the two jets is more pronounced. At that particular station, the discrepancies between the measured and the current values are higher. This might be due to either insufficient grid resolution in the longitudinal direction or inefficiencies of the turbulence model. This is more evident at the mid-distance between the two jets. Further downstream the velocity maximum near the wall on the two middle planes disappears and a boundary layer forms. However, at x/D=10 the u-profile in the plane z/D=2 shows that high velocities exist close to the wall. At that point, the flow close to the wall assumes wall-jet character.

The v-profiles, shown in Figure 5, suggest a very complex secondary motion downstream of the exit. It is noticeable that at z/D=2 the v-velocities have negative values, indicating that air is sucked in that region from the freestream flow. At x/D=4.5 the jet is not bent over, as the high positive v-velocities on the central planes of the jet suggest. Clearly, at this station, the wake region is not close to the wall, as the near-wall region is occupied by a wall-jet flow. Like the single-jet case, these wake-regions induce downward motion of the fluid above them. However, beneath the wake regions, an upward motion of the fluid is induced, which is enhanced by the presence of the strong bound motion. This upward motion carries higher-momentum fluid from the wall-jet flow upwards to remove the momentum deficit in the wake. Contrary to the single-jet case [12], very close to the wall the v-velocity component does take negative values. This indicates that there does not exist a vortex counterrotating the bound vortex.

Finally, the temperature profiles are plotted in Figure 6. Corresponding cooling efficiencies of the blade-hole system are determined as the potential ratio of temperature differences.

$$\eta = \frac{T_{windtunnel} - T_{avg.blade\_temp}}{T_{windtunnel} - T_{jet\_temp}} \qquad (11)$$

Table 1 documents cooling effect for the following four jet cooling numerical experiments.

(a) α=45° R=3, L=42.0 - 2*r;
(b) α=45° R=2, L=42.0 - 2*r;
(c) α=30° R=3, L=42.0 - 2*r; and
(d) α=15° R=3, L=21.0 - r.

Evidently, the higher blow ratio shows more cooling effect. As the flow angle α and the hole spacing L decrease, the secondary vortex structure forces the cool jet to bend and hit the blade more effectively, hence improve the cooling efficiency.

Table 1.

Cooling Efficiency	Case (a)	Case (b)	Case (c)	Case (d)
η	10%	4%	28%	55%

CONCLUSIONS

The computational experiments suggest maximum effectiveness of the jet cooling as a direct result of the presence of a row of holes and the ensuing jet angle. Smaller jet angle and reduced hole spacing improves the cooling efficiency. The size of the velocity components induced by the bound vortices depends on the magnitude of vorticity and the distance from the core of the vortex. When the bound vortices are restrained

spatially by the row of jets, the induced velocities are high and more jet air is brought towards the wall. The interaction between neighboring jets enhances turbulence intensity upstream of the jets and therefore promotes the diffusion of the jet into the mainstream flow. More analyses should be done to find an optimum L and α for maximum cooling efficiency.

REFERENCES

1. R. Jordison, Flow in a jet directed normal to the wind, *Aero. Res. Council, R & M.*, No. 3074, 1958.
2. R. Fearn and R. P. Weston, Vorticity associated with a jet in a cross flow, *AIAA J.*, Vol. 12, pp. 1666-1671, 1974.
3. Z. M. Moussa, J. W. Trischka and S. Eskinazi, The near field in the mixing of a round jet with a cross-stream, *J. Fluid. Mechanics*, Vol. 80, pp. 49-80, 1977.
4. J. Andreopoulos and W. Rodi, Experimental investigation of jets in a crossflow, *J. Fluid. Mechanics*, Vol. 138, pp. 93-127, 1984.
5. Y.M Vizel and I. L. Mostinskii, Deflection of a jet injected into a stream, *Fluid Dyn..*, Vol. 8, pp. 127-139, 1965.
6. C. L. H. Chen, Aufrollung eines zylindrischen strahles durch querwind, Doctoral Thesis, University of Gottingen, 1942.
7. D. Adler and A. Baron, Prediction of a three-dimensional circular turbulent jet in a crossflow, *AIAA J.*, Vol. 17, pp. 168-174, 1979.
8. J. C. Chien and J. A. Schetz, Numerical solution of the three dimensional Navier-Stokes equations with applications to channel flows and a buoyant jet in a cross flow, *ASME J. Appl.. Mech..*, Vol. 42, pp. 575-579, 1975.
9. A. A. Amer, B. A. Jubran and M. A. Hamdan, Comparison of different two-equation turbulence models for prediction of film cooling from two rows of holes, *Numer. Heat Transfer, Part A*, Vol. 21, pp. 143-162, 1992.
10. M. M. Rai, Navier-Stokes simulations of blade-vortex interaction using high-order accurate upwind schemes, AIAA Paper 87-0543, 1987.
11. P. Tamamidis and D. N. Assanis, Three-dimensional incompressible flow calculations with alternative discretization schemes, *Numer. Heat Transfer, Part B*, Vol. 24, pp. 57-76, 1993.
12. P. Tamamidis and S. Roy, Numerical investigation of the isothermal flow field generated by single and multiple jets issuing at an angle of 45° into an incompresible horizontal cross flow, *J. Fluid Engineering*, in press 1998.

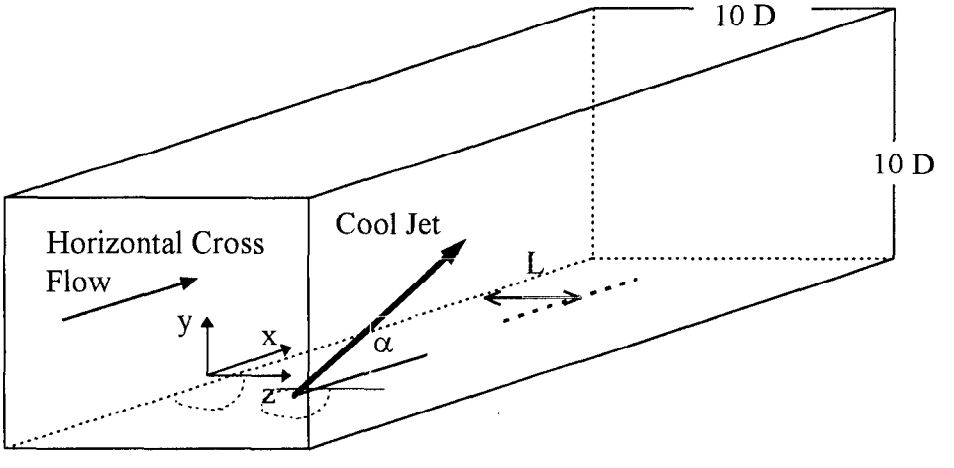

Figure 1: Schematic of the flow domain for the multiple-jet case

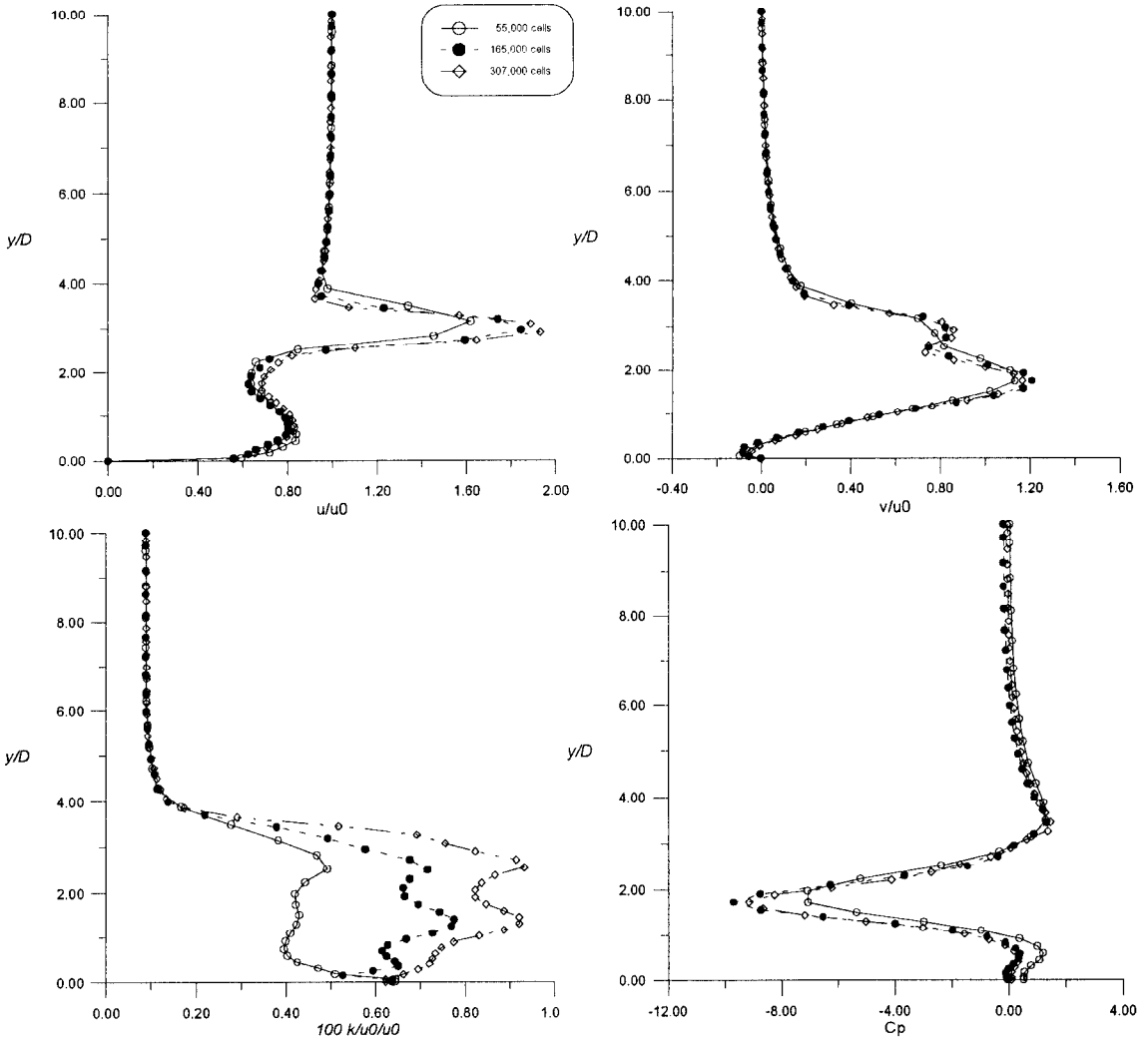

Figure 2: Grid independence studies at x/D=4.5 and z/D=0 [12].

a) Velocity vectors : sectional view

b) Temperature contours : sectional view

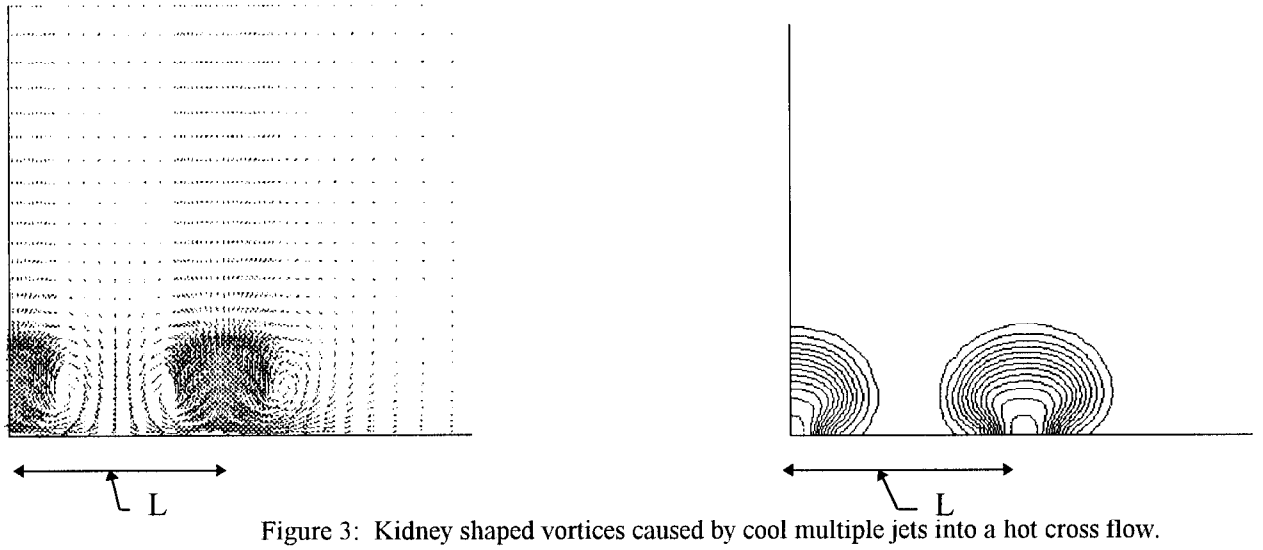

Figure 3: Kidney shaped vortices caused by cool multiple jets into a hot cross flow.

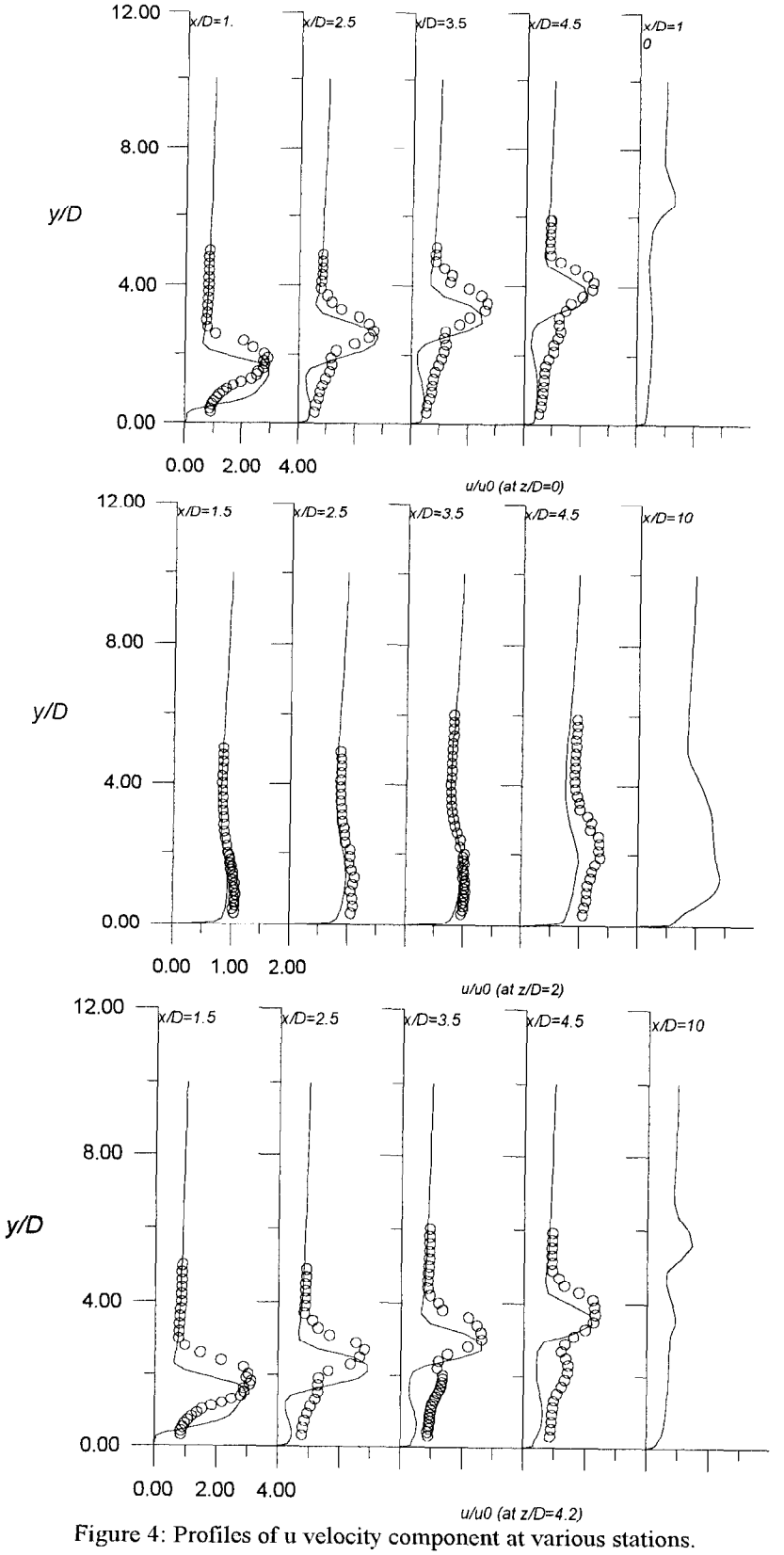

Figure 4: Profiles of u velocity component at various stations.

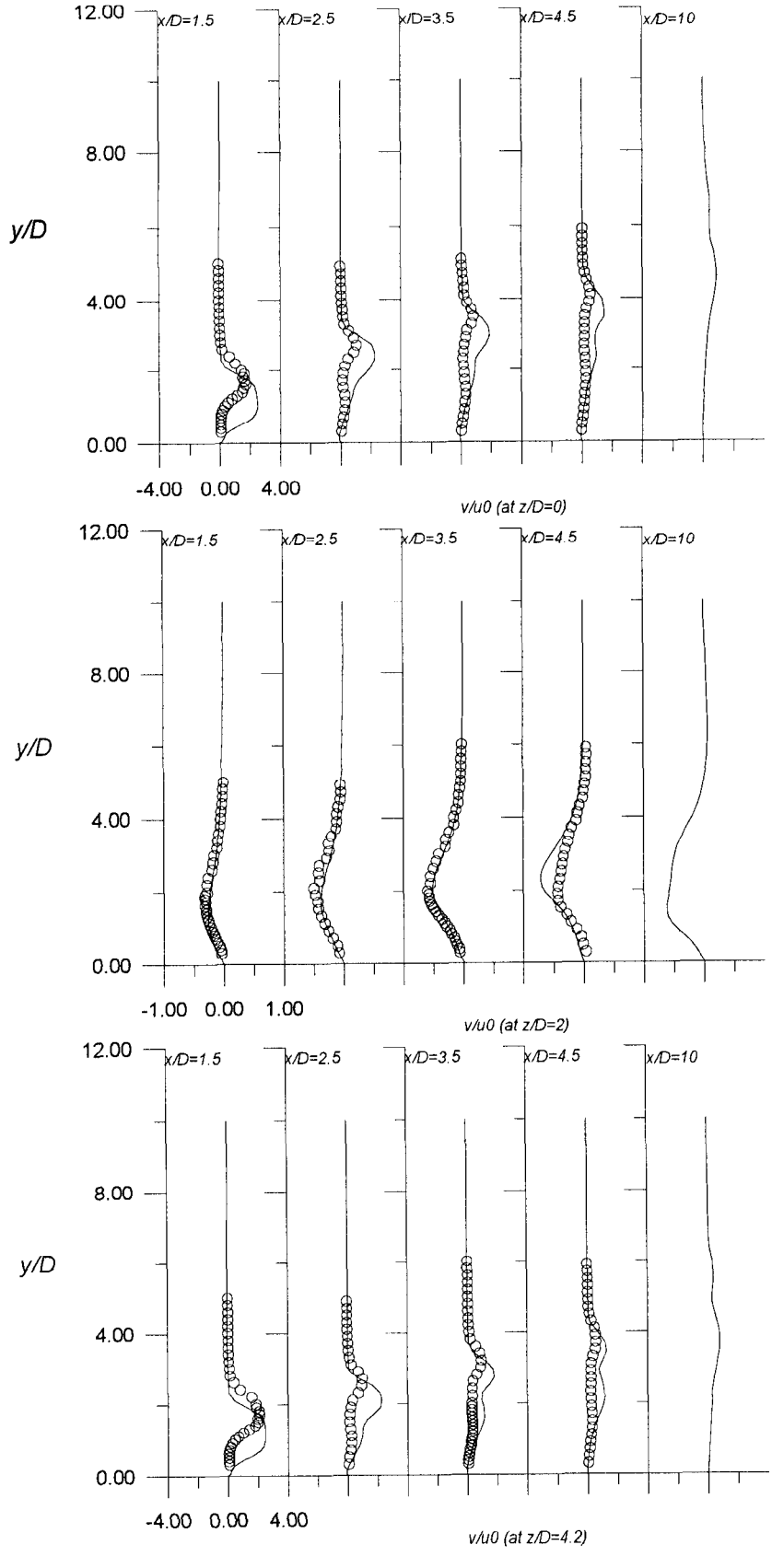

Figure 5: Profiles of v velocity components at various stations.

a) Turbine blade : bottom section

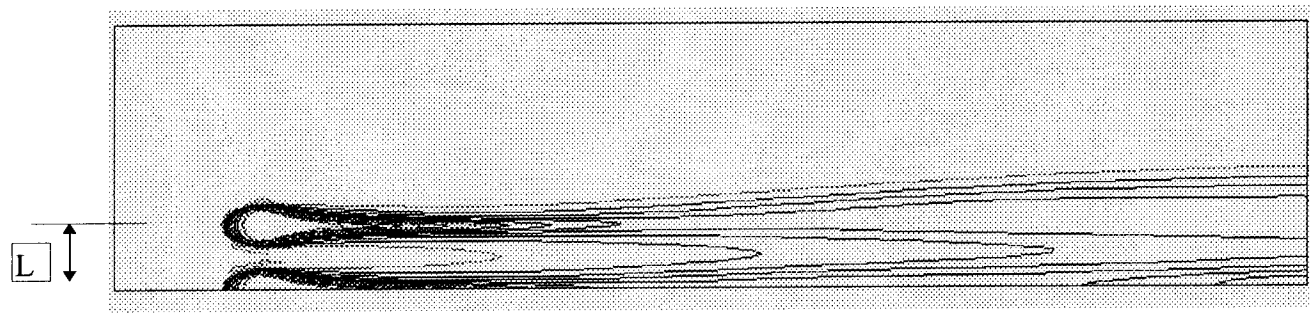

b) Turbine blade : normal to the mid-plane

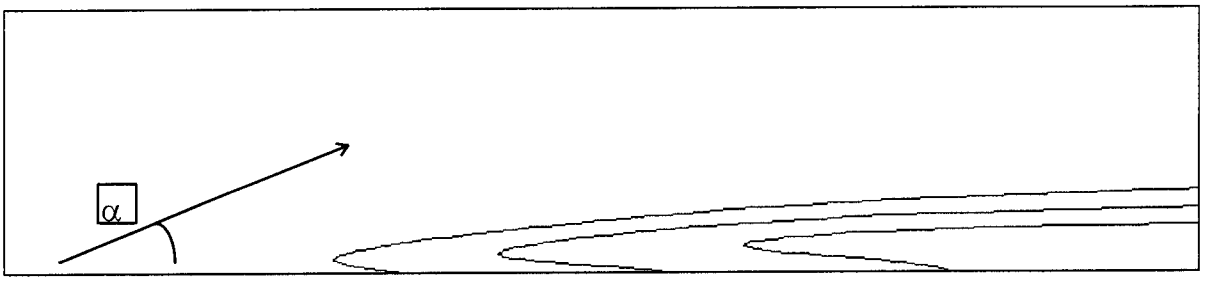

c) Perspective view

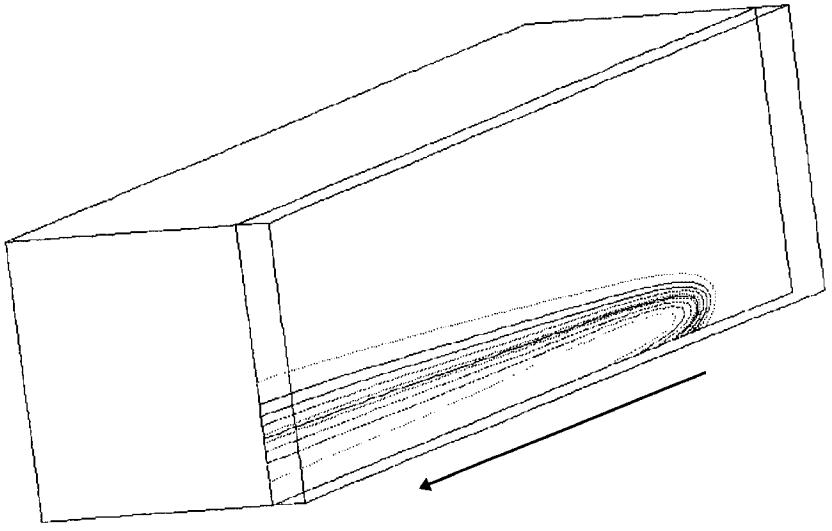

Figure 6: Thermal contours on the plane cut along the middle of the jets show downstream spread of the cooling effect.